BIOCELL

Tech Science Press

http://doi.org/10.32604/biocell.2026.080414

ARTICLE

YOD1 Stabilizes RIPK1 via Deubiquitination to Activate NF-κB and Promote Cardiomyocyte H/R Injury

Liangliang Liu, Linjun Wang, Xin Song and Zhen Liu*

Department of Cardiology, Lianyungang Hospital of Traditional Chinese Medicine, Lianyungang, China
*Corresponding Author: Zhen Liu. Email: 19805083038@163.com

Received: 09 February 2026; Accepted: 13 May 2026; Published: 26 August 2026

ABSTRACT: Background: Myocardial ischemia-reperfusion (I/R) injury represents a severe pathological process in cardiovascular diseases. This study aims to elucidate the mechanism of the yeast ovarian tumor (OTU) domain-containing protein 1 (YOD1) in cardiomyocyte injury. **Methods:** A hypoxia/reoxygenation (H/R) model was established using human AC16 cells to simulate I/R injury *in vitro*. Reverse transcription quantitative PCR (RT-qPCR) and western blotting were used to detect gene and protein expression. Cellular functions were evaluated using Cell Counting Kit-8 (CCK-8), lactate dehydrogenase (LDH), enzyme-linked immunosorbent assay (ELISA), flow cytometry, and biochemical kits. Protein interaction was validated through co-immunoprecipitation (Co-IP), ubiquitination assays, and cycloheximide (CHX) chase experiments. **Results:** YOD1 was up-regulated in H/R-induced AC16 cells ($p < 0.01$). H/R decreased cell viability ($p < 0.001$), superoxide dismutase (SOD) ($p < 0.001$), and glutathione peroxidase 4 (GPX4) ($p < 0.001$) and increased LDH ($p < 0.001$), interleukin-6 (IL-6) ($p < 0.001$), tumor necrosis factor-alpha (TNF-α) ($p < 0.001$), reactive oxygen species (ROS) ($p < 0.001$), malondialdehyde (MDA) ($p < 0.001$), and Fe^{2+} ($p < 0.001$); these effects were alleviated by YOD1 knockdown ($p < 0.01$). YOD1 knockdown ($p < 0.001$) also reversed H/R-increased receptor-interacting serine/threonine kinase 1 (RIPK1) protein levels ($p < 0.001$) and p-p65/p65 ($p < 0.001$) and p-nuclear factor-kappa-B inhibitor alpha (p-IκBα)/IκBα ($p < 0.001$) ratios. RIPK1 overexpression reversed the protective effects of YOD1 knockdown via activating the nuclear factor-kappa-B (NF-κB) pathway ($p < 0.01$). Mechanistically, YOD1 interacted with RIPK1 and inhibited its K63-linked ubiquitination degradation ($p < 0.01$). These statistical significances support the clinical potential of targeting YOD1 to mitigate inflammation, oxidative stress, and ferroptosis-related changes in myocardial I/R injury. **Conclusion:** YOD1 stabilizes RIPK1 via K63-linked ubiquitination to activate the NF-κB pathway, exacerbating inflammation, oxidative stress, and ferroptosis-related changes in H/R-induced cardiomyocytes. YOD1 may represent a potential therapeutic target for myocardial I/R injury, though further *in vivo* and clinical validation is required.

KEYWORDS: Yeast ovarian tumor domain-containing protein 1; receptor-interacting serine/threonine kinase 1; myocardial ischemia-reperfusion injury; ubiquitination; ferroptosis; nuclear factor-kappa-B pathway

1 Introduction

Myocardial ischemia-reperfusion (I/R) injury is a central pathological event in cardiovascular disease management, commonly occurring following thrombolysis for acute myocardial infarction or coronary artery bypass grafting. Its essence lies in secondary tissue damage triggered by the restoration of blood flow after ischemic hypoxia [1]. Although reperfusion is a critical measure for salvaging myocardial tissue, approximately 50% of myocardial infarction patients still experience progressive decline in cardiac function following revascularization, ultimately progressing to heart failure or even death [2]. Current

research indicates that myocardial I/R injury involves a complex molecular network, including dysregulated inflammatory responses, oxidative stress surges, and abnormal activation of cell death pathways [3,4]. Among these, inflammatory cytokine storms, overproduction of reactive oxygen species (ROS), and ferroptosis are considered core drivers of injury progression [5,6]. However, the precise regulatory mechanisms behind these pathologies are still unclear, and identifying novel intervention targets remains a key research focus in this field.

Yeast ovarian tumor (OTU) domain-containing protein 1 (YOD1) is a conserved deubiquitinase (DUB) belonging to the OTU domain protease family [7]. It was initially identified as a component of the endoplasmic reticulum-associated degradation pathway [8]. Recent studies reveal its pivotal role in regulating substrate protein stability across various diseases [9], including cancer [10], neurological disorders [11], and inflammatory conditions [12]. Reports indicated that YOD1 expression levels were elevated in human hypertrophic myocardial tissues and mouse models, while YOD1 knockdown suppressed cardiac hypertrophy [13]. However, the specific role of YOD1 in myocardial I/R injury and its regulatory mechanisms remains poorly understood.

Nuclear factor-kappa-B (NF-κB) pathway, a common pro-inflammatory pathway [14,15], is extensively activated during I/R injury. It amplifies the damaging effects by up-regulating inflammatory factor expression, promoting oxidative stress responses, and regulating cell death processes [16]. Receptor-interacting serine/threonine kinase 1 (RIPK1), acting as an upstream regulatory node of the NF-κB pathway [17]; its abnormal activation can aggravate cardiomyocyte injury through inflammasome formation and downstream signaling [18]. Notably, RIPK1 stability is tightly regulated by ubiquitination. Ubiquitination-mediated degradation suppresses its function, while deubiquitination enhances its activity by stabilizing protein levels [19]. RIPK1 is up-regulated in myocardial I/R mice, serving as a potential marker of necrosis [20]. Furthermore, targeting RIPK1-mediated necrotic apoptosis, oxidative stress, and ferroptosis represents a novel multi-target therapeutic approach for ischemic stroke [21]. More importantly, this study predicted through online databases that RIPK1 was a substrate of YOD1.

Based on this, the present study utilizes the hypoxia/reoxygenation (H/R)-induced human myocardial cell line AC16 as a model to investigate whether YOD1 modulates RIPK1 expression to exert effects in myocardial I/R injury. This research aims to investigate the molecular mechanisms of YOD1 in H/R-induced cardiomyocyte injury, providing preliminary insights that may inform future studies on myocardial I/R injury.

2 Methods

2.1 Cell Culture and H/R Model Establishment

The human cardiac cell line AC16 was provided by Guangzhou Yuanjing Biotechnology Co., Ltd. (Guangzhou, China). Cells were routinely maintained in Dulbecco's modified Eagle medium (Beyotime, Shanghai, China), supplemented with 10% fetal bovine serum (Huankai, Guangzhou, China) and 1% penicillin/streptomycin (Oumarsi, Shanghai, China) at 37°C with 5% CO_2. The cell line was authenticated via short tandem repeat (STR) profiling and verified to be mycoplasma-free.

Establishment of the H/R models: To simulate *in vivo* I/R injury, AC16 cells were placed in a hypoxic incubator (1% O_2, 5% CO_2, 94% N_2) for 6 h. After replacement with fresh culture medium, cells were further incubated under normoxic conditions (95% O_2, 5% CO_2) for 12 h. This protocol was selected based on preliminary experiments comparing various hypoxia durations (3–24 h) and reoxygenation durations (6–24 h), where 6 h hypoxia/12 h reoxygenation reproducibly reduced cell viability to approximately 50–60% of control levels without causing excessive cell death (viability < 30%), making it suitable for evaluating

protective effects. The 1% O_2 concentration is a well-established standard for simulating myocardial ischemic hypoxia that effectively leads to hypoxia-inducible factor-1α (HIF-1α) stabilization and subsequent hypoxic responses [22]. AC16 cells, as a human-derived cardiomyocyte line, provide a consistent genetic background and phenotype for mechanistic studies, and this H/R protocol has been widely used to model myocardial I/R injury *in vitro* [23]. Control cells were maintained under normoxic conditions throughout the experiment.

2.2 Cell Transfection

To silence YOD1, small interfering RNA (siRNA) targeting YOD1 (siYOD1) and negative control (siNC) were transfected into AC16 cells using Hieff Trans® Universal Transfection Reagent (40808ES, Yeasen, Shanghai, China). Subsequent experiments were conducted 48 h post-transfection. To overexpress RIPK1, RIPK1 overexpression plasmids (RIPK1) and control vector plasmids were introduced into AC16 cells using the same method. The above siRNAs and overexpression vector plasmids were obtained from Genscript (Nanjing, China).

2.3 Reverse Transcription Quantitative PCR (RT-qPCR)

AC16 cells were treated with TRIzol reagent (ZN00801, Shinegene, Shanghai, China) to extract RNA. RNA concentration and purity were evaluated via the A260/280 absorbance ratio on a NanoDrop spectrophotometer (Thermo Fisher Scientific, Waltham, MA, USA). Specimens with a ratio of 1.8–2.0 proceeded to subsequent analysis. For reverse transcription, total RNA (1 μg) was mixed with reagents from the PrimeScript RT Kit (RR037A, Takara, Beijing, China) based on the manufacturer's specifications. qPCR amplification was conducted using SYBR Green Premix Pro Taq HS Mix (AG11718, Accurate Biology, Changsha, China) on a QuantStudio 5 real-time quantitative PCR instrument (Applied Biosystems, Carlsbad, CA, USA). The thermal cycling conditions were as follows: initial denaturation at 95°C for 30 s, followed by 40 cycles of denaturation at 95°C for 5 s and annealing/extension at 60°C for 34 s. To confirm primer specificity, a melt curve analysis was conducted after amplification cycles following the conditions: 95°C for 15 s, 60°C for 1 min, followed by a gradual temperature increase from 60°C to 95°C at a rate of 0.15°C/s. Glycerol-3-phosphate dehydrogenase (GAPDH) was used for normalization. Each reaction was carried out in triplicate. Gene expression levels were confirmed with the $2^{-\Delta\Delta Ct}$ approach. Primer sequences are exhibited in Table 1.

Table 1: RT-qPCR primer sequence.

Gene	Forward (5′–3′)	Reverse (5′–3′)
YOD1	TTCGCGCTTGCTAAGGTACT	AAACATCGCGAGAAGTTGCG
GAPDH	GACAGTCAGCCGCATCTTCT	GCGCCCAATACGACCAAATC

2.4 Western Blotting

AC16 cells were lysed with radioimmunoprecipitation assay (RIPA) lysis buffer (P0013B, Beyotime) for total protein extraction. Protein concentration was evaluated with the bicinchoninic acid assay method (PC0020, Solarbio, Beijing, China). Following separation via sodium dodecyl sulfate-polyacrylamide gel electrophoresis (SDS-PAGE), the protein was electrotransferred to polyvinylidene fluoride membranes (Beyotime). Following blocking with 5% skim milk (Beyotime), the proteins were exposed to primary antibodies of YOD1 (1:1000, ab269141, Abcam, Cambridge, UK), RIPK1 (1:1000, ab300617, Abcam), glutathione peroxidase 4 (GPX4, 1:5000, ab125066, Abcam), acyl-CoA synthetase long chain family member 4 (ACSL4, 1:20,000, ab155282, Abcam), p65 (1:10,000, ab32536, Abcam), p-p65 (1:1000, ab76302, Abcam),

IκBα (1:1000, #4812, Cell signaling technology, Danvers, MA, USA), p-IκBα (1:1000, #2859, Cell signaling technology), nuclear marker Histone H3 (1:3000, ab1791, Abcam), and the housekeeping gene GAPDH (1:10,000, ab181602, Abcam) at 4°C for 12 h. Then, reaction with HRP-labeled secondary antibody (1:10,000, ab6721, Abcam) was conducted at 37°C for 1 h. The image was developed with an enhanced chemiluminescent kit (P0018M, Beyotime) and analyzed for grayscale values using the ImageJ 1.47 software (NIH, Bethesda, MD, USA). Proteins from different cellular compartments were fractionated into nuclear and cytoplasmic portions with the aid of the Nuclear and Cytoplasmic Protein Extraction Kit (P0028, Beyotime).

2.5 Cell Viability Measurement

AC16 cells were spread into a 96-well plate with 1×10^4 cells/well. Following exposure to H/R or/and transfection of siRNAs and overexpression vectors as required, cells were exposed to Cell Counting Kit-8 (CCK-8) solution (10 μL, 40203ES60, Yeasen). After a 2-h incubation, absorbance at 450 nm was detected via a SpectraMax® M microplate reader (Molecular Devices, Shanghai, China).

2.6 Lactate Dehydrogenase (LDH) Release Detection

LDH release was measured by applying the LDH Assay Kit (C0016, Beyotime) to assess the extent of cellular damage. Briefly, the cells treated with different conditions were treated with the LDH release solution for 1 h. After centrifugation at 400× *g* for 5 min using a MPC2000 96-well plate centrifuge (DHS, Tianjin, China), the supernatant was collected and aliquoted into a 96-well plate for subsequent detection. Then, 60 μL of the LDH detection working solution was introduced and reacted at 25°C for 30 min in the dark. The absorbance at 490 nm was measured using a SpectraMax® M microplate reader (Molecular Devices).

2.7 Inflammatory Cytokine Testing

Interleukin-6 (IL-6) and tumor necrosis factor-α (TNF-α) levels in cell supernatants were quantified using the Human enzyme-linked immunosorbent assay (ELISA) Kits (97068ES96 and 97072ES96, Yeasen). After collecting the cell supernatants for analysis, standard and test samples were applied to the corresponding microplate wells and incubated at 37°C for 2 h. Subsequently, the enzyme conjugate was introduced and incubated for 20 min at 37°C. Next, the substrate solution was applied, followed by a 15-min color development period. After the reaction was terminated, absorbance was assessed at 450 nm with a SpectraMax® M microplate reader (Molecular Devices).

2.8 Lipid ROS Levels

Lipid ROS levels were examined with BODIPY 581/591 C11 probe (S0043S, Beyotime) via flow cytometry. Cells were harvested, resuspended, and incubated with the probe staining working solution at 37°C for 20 min. Subsequent analysis was performed with a BD BD FACSDiscover™ S8 flow cytometer (BD Biosciences, Franklin Lakes, NJ, USA).

2.9 Malondialdehyde (MDA) Levels

Following cell lysis with RIPA lysis buffer (Beyotime), the supernatant was harvested. Cell homogenate, lysate, and standards were introduced into separate centrifuge tubes for testing. Subsequently, the MDA assay working solution (S0131S, Beyotime) was introduced and heated at 100°C for 15 min. After cooling, absorbance at 532 nm was tested with a SpectraMax® M microplate reader (Molecular Devices). MDA content was calculated based on the protein concentration.

2.10 Superoxide Dismutase (SOD) Levels

Cells were lysed employing the sample preparation solution from the Total Superoxide Dismutase Assay Kit with WST-8 (S0101S, Beyotime), and supernatant was collected for subsequent detection. Each well received the test specimen, SOD detection buffer, WST-8/enzyme working solution, and/or reaction initiation working solution. After reacting at 37°C for 30 min, the absorbance at 450 nm was tested.

2.11 Fe^{2+} Levels

Fe^{2+} levels were detected with a Ferric and Ferrous Ion Assay Kit (S1066S, Beyotime). Cell lysis, applying the buffer from the kit, was conducted in a TissueMaster™ High-Throughput Tissue Homogenizer (Beyotime). The supernatant was collected for protein concentration measurement and subsequent assays. Hydrochloric acid was introduced to the collected samples and reacted at 60°C for 30 min. The supernatant was used as the test sample. Standard solutions were prepared at different concentrations to make a standard curve. The sample, Reduction Buffer, and Decontamination Solution were introduced to the corresponding wells of a 96-well plate. Subsequently, Iron Probe was used to treat samples at 37°C for 30 min. Absorbance at 593 nm was recorded on a SpectraMax® M microplate reader (Molecular Devices), and Fe^{2+} concentration was confirmed using the standard curve.

2.12 Co-Immunoprecipitation (Co-IP) and Ubiquitination Detection

Cell lysis was conducted using pre-cooled Cell lysis buffer for Western and IP (Beyotime) on an orbital shaker at 4°C and 120 rpm for 30 min. After centrifugation, a small portion of the total protein lysate was used as the "Input" control. The remaining protein samples were probed with specific antibodies for IP at 4°C for 12 h: anti-RIPK1 (1:30, ab300617, Abcam)/anti-YOD1 (1:30, ab269141, Abcam) or normal IgG (1:50, ab172730, Abcam) as a negative control. Subsequently, Protein A/G magnetic beads (Vazyme, Nanjing, China) were introduced and reacted at 4°C for 4 h to make the antibody-protein-bead complex. After washing and eluting, SDS-PAGE loading buffer (Beyotime) was introduced into the magnetic beads, followed by heating at 100°C for 10 min. Supernatant was then employed for Western blotting analysis.

For Co-IP, the proteins were combined with anti-RIPK1 (1:1000, ab300617, Abcam) or anti-YOD1 (1:1000, ab269141, Abcam) to verify the interaction.

For the ubiquitination assay, the proteins were combined with anti-RIPK1 (1:1000, ab300617, Abcam) and anti-ubiquitin (1:5000, 10201-2-AP, Proteintech, Wuhan, China) to assess the ubiquitination status of RIPK1.

2.13 Cycloheximide (CHX) Chase Experiments

CHX (50 μg/mL, MB2208-1, MeilunBio, Dalian, China) was added to H/R-induced AC16 cells transfected with siYOD1 or siNC. After CHX exposure for 0 h, 2 h, 4 h, and 6 h, cells were used for RIPK1 protein degradation by western blotting.

2.14 Statistical Method

All experiments were independently carried out with three biological replicates ($n = 3$), each comprising three technical replicates. Data are represented as mean ± standard deviation. Statistical analyses were carried out with GraphPad Prism 8.0 software. Unpaired *t*-tests compared two groups, while one-way analysis of variance with Tukey's post hoc test compared three or more groups. $p < 0.05$ was taken to indicate statistical significance.

3 Results

3.1 YOD1 Knockdown Alleviates Inflammation, Oxidative Stress, and Ferroptosis-Associated Alterations in H/R-Treated AC16 Cells

To better explore the role of YOD1 in I/R, this study first examined its expression. Compared with the control AC16 cells, YOD1 was up-regulated in H/R-treated AC16 cells (Fig. 1A,B). Silencing of YOD1 reversed H/R-induced YOD1 up-regulation (Fig. 2A). The reduction in cellular viability and the elevation in LDH, IL-6, and TNF-α levels caused by H/R were restored in AC16 cells after YOD1 knockdown (Fig. 2B–E). Besides, under the H/R context, the elevated lipid ROS and MDA levels and the reduced SOD levels were mitigated by YOD1 down-regulation (Fig. 2F–H). Additionally, intracellular Fe^{2+} levels were up-regulated after H/R exposure, which were further decreased with YOD1 silencing (Fig. 2I). Western blotting analysis in Fig. 2J revealed that H/R stimulation decreased GPX4 expression and increased ACSL4 expression relative to the Control group. Notably, YOD1 knockdown reversed these changes, enhancing GPX4 expression and suppressing ACSL4 expression. Taken together, these findings demonstrate that YOD1 silencing alleviates H/R-induced cell injury by suppressing inflammation, lipid peroxidation, and ferroptosis-associated alterations, while enhancing antioxidant capacity.

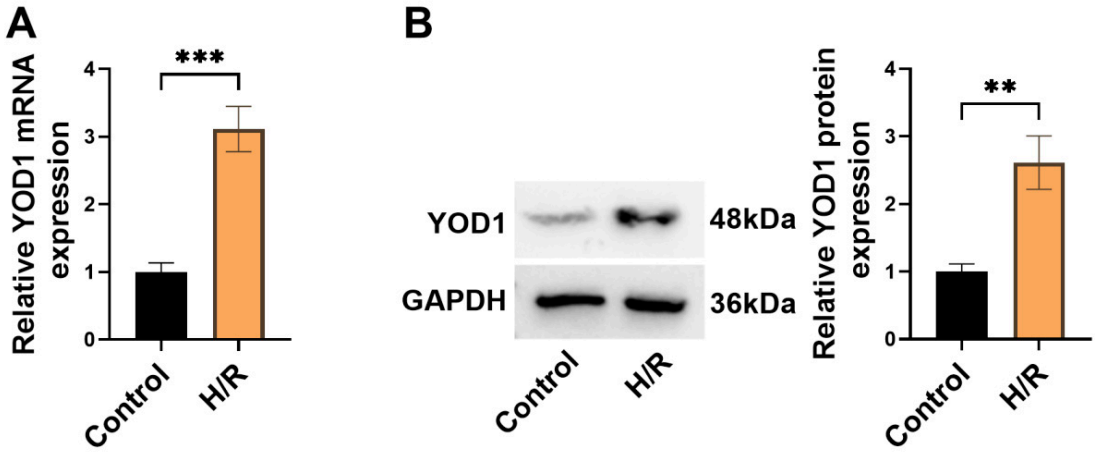

Figure 1: YOD1 is highly expressed in H/R-induced AC16 cells. (**A**,**B**) YOD1 mRNA and protein expression in control and H/R-induced AC16 cells were detected by RT-qPCR and western blotting assays. Data are presented as mean ± SD from three independent experiments ($n = 3$). $^{**}p < 0.01$, $^{***}p < 0.001$.

3.2 Knockdown of YOD1 Inhibits RIPK1 Expression and Blocks the NF-κB Signaling Pathway in H/R-Treated AC16 Cells

To explore whether YOD1 regulates RIPK1 expression during H/R, western blotting was performed to detect RIPK1 protein levels. The results revealed that the elevation of RIPK1 levels induced by H/R stimulation was markedly reduced by YOD1 knockdown (Fig. 3A). Additionally, YOD1 knockdown significantly suppressed H/R-induced elevation in p-p65/p65 and p-IκBα/IκBα ratios (Fig. 3B). Furthermore, nuclear-cytoplasmic separation assays revealed that H/R stimulation promoted p65 nuclear translocation, which was markedly inhibited by YOD1 knockdown (Fig. S1). Collectively, YOD1 knockdown mitigates H/R-induced up-regulation of RIPK1 and suppresses NF-κB pathway activation, suggesting that YOD1 may be a crucial regulator in H/R-triggered cellular responses.

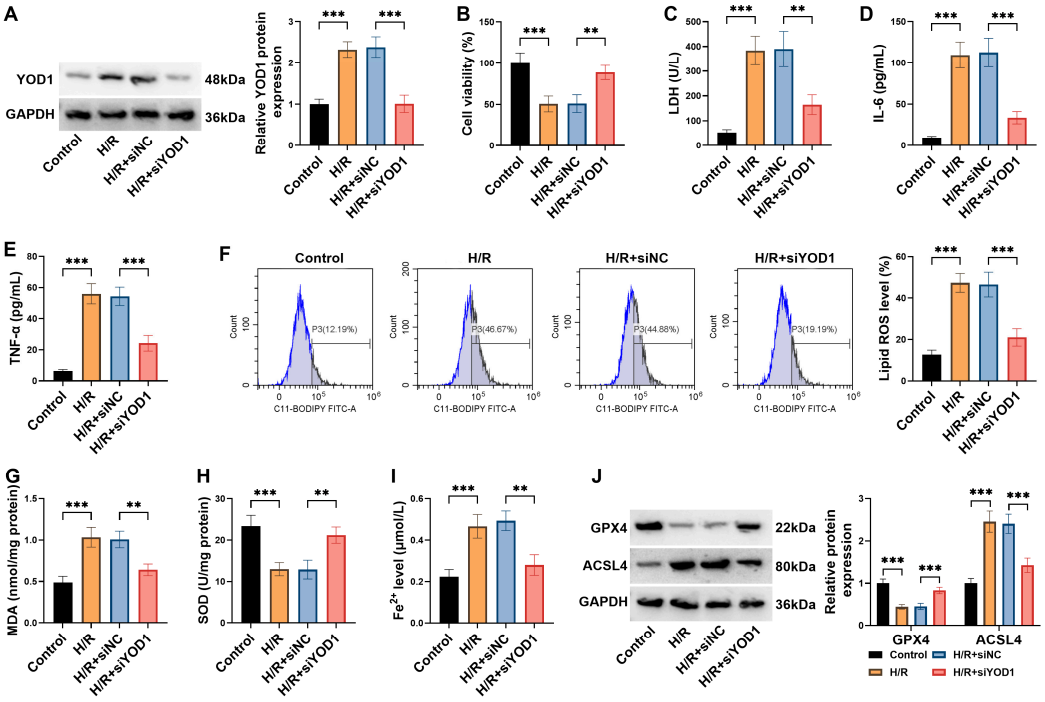

Figure 2: Knockdown of YOD1 alleviates inflammation, oxidative stress, and ferroptosis-associated alterations in H/R-induced AC16 cells. (**A**) YOD1 protein expression in AC16 cells with Control, H/R, H/R+siNC, and H/R+siYOD1 groups was detected by western blotting assay. (**B**) The viability of AC16 cells with Control, H/R, H/R+siNC, and H/R+siYOD1 groups was detected by CCK-8 assay. (**C**) LDH release levels in AC16 cells with Control, H/R, H/R+siNC, and H/R+siYOD1 groups were detected using the relevant kit. (**D**,**E**) IL-6 and TNF-α levels in AC16 cells with Control, H/R, H/R+siNC, and H/R+siYOD1 groups were detected by ELISA. (**F**) Lipid ROS levels in AC16 cells with Control, H/R, H/R+siNC, and H/R+siYOD1 groups were detected by flow cytometry. (**G**–**I**) MDA, SOD, and Fe^{2+} levels in AC16 cells with Control, H/R, H/R+siNC, and H/R+siYOD1 groups were detected by relevant kits. (**J**) GPX4 and ACSL4 protein expression in AC16 cells with Control, H/R, H/R+siNC, and H/R+siYOD1 groups was detected by western blotting assay. Data are presented as mean ± SD from three independent experiments (n = 3). $^{**}p < 0.01$, $^{***}p < 0.001$.

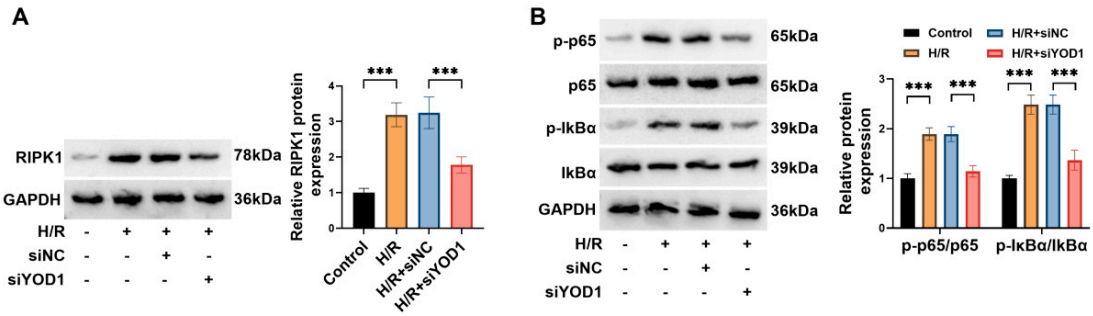

Figure 3: Knockdown of YOD1 inhibits the expression of RIPK1 and blocks the NF-κB signaling pathway in H/R-induced AC16 cells. (**A**) RIPK1 protein expression in AC16 cells with Control, H/R, H/R+siNC, and H/R+siYOD1 groups was detected by western blotting assay. (**B**) p-p65/p65 ratio and p-IκBα/IκBα ratio in AC16 cells with Control, H/R, H/R+siNC, and H/R+siYOD1 groups were detected by western blotting assay. Data are presented as mean ± SD from three independent experiments (n = 3). $^{***}p < 0.001$.

3.3 Overexpression of RIPK1 Reverses the Effect of YOD1 Knockdown on H/R-Exposed AC16 Cells

To further explore the effects of RIPK1 in H/R-induced injury and its regulation by YOD1, a series of experiments was performed. Western blotting analysis revealed that RIPK1 protein was markedly increased with RIPK1 overexpression (Fig. 4A). Knockdown of YOD1 alleviated the decrease in cell viability and the increase in LDH release in H/R-exposed AC16 cells. Conversely, RIPK1 overexpression abrogated the protective effects of YOD1 knockdown, leading to further decreases in cell viability and increases in LDH release (Fig. 4B,C). Under H/R context, RIPK1 overexpression abolished the inhibitory effects of YOD1 knockdown on IL-6 and TNF-α levels (Fig. 4D). Moreover, YOD1 knockdown mitigated the increases in lipid ROS, MDA, and Fe^{2+} levels and the decreases in SOD levels caused by H/R stimulation, while RIPK1 overexpression reversed these phenomena (Fig. 4E–H). H/R reduced the expression of GPX4 and increased ACSL4, but these changes were reversed with YOD1 knockdown. Notably, RIPK1 overexpression abrogated these effects of YOD1 knockdown, reducing GPX4 levels and increasing ACSL4 expression (Fig. 4I). Furthermore, under the H/R context, the inhibitory effects of YOD1 silencing on the ratios of p-p65/p65 and p-IκBα/IκBα were restored after RIPK1 overexpression (Fig. 4J). These results demonstrate that YOD1 knockdown protects against H/R-induced injury by regulating RIPK1, which in turn mitigates inflammation, oxidative stress, ferroptosis-associated alterations, and NF-κB pathway activation.

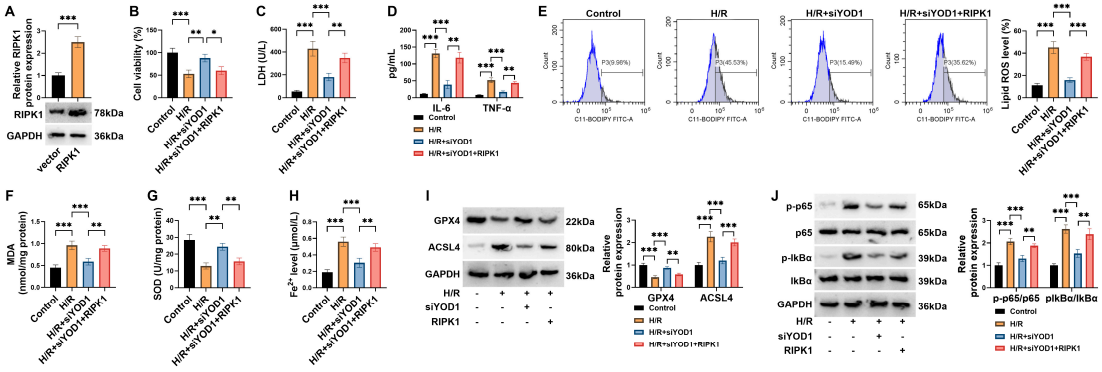

Figure 4: Overexpression of RIPK1 reverses the effect of YOD1 knockdown on H/R-induced AC16 cells. (**A**) RIPK1 protein expression in AC16 cells with the vector and RIPK1 groups was detected by western blotting assay. (**B**) The viability of AC16 cells with Control, H/R, H/R+siYOD1, and H/R+siYOD1+RIPK1 groups was detected by CCK-8 assay. (**C**) LDH release levels in AC16 cells with Control, H/R, H/R+siYOD1, and H/R+siYOD1+RIPK1 groups were detected using a relevant kit. (**D**) IL-6 and TNF-α levels in AC16 cells with Control, H/R, H/R+siYOD1, and H/R+siYOD1+RIPK1 groups were detected by ELISA. (**E**) Lipid ROS levels in AC16 cells with Control, H/R, H/R+siYOD1, and H/R+siYOD1+RIPK1 groups were detected by flow cytometry. (**F**–**H**) MDA, SOD, and Fe^{2+} levels in AC16 cells with Control, H/R, H/R+siYOD1, and H/R+siYOD1+RIPK1 groups were detected by relevant kits. (**I**) GPX4 and ACSL4 protein expression in AC16 cells with Control, H/R, H/R+siYOD1, and H/R+siYOD1+RIPK1 groups was detected by western blotting assay. (**J**) p-p65/p65 ratio and p-IκBα/IκBα ratio in AC16 cells with Control, H/R, H/R+siYOD1, and H/R+siYOD1+RIPK1 groups were detected by western blotting assay. Data are presented as mean ± SD from three independent experiments ($n = 3$). $^{*}p < 0.05$, $^{**}p < 0.01$, $^{***}p < 0.001$.

3.4 YOD1 Inhibits the Ubiquitination Levels of RIPK1

To determine whether YOD1 interacts with RIPK1, a Co-IP assay was performed. As shown in Fig. 5A, the results confirmed that endogenous YOD1 physically interacted with RIPK1. Further, under H/R conditions, YOD1 knockdown promoted K63-linked ubiquitination of RIPK1 (Fig. 5B and S2). The CHX chase assays further demonstrated that in the H/R+siYOD1 group, RIPK1 protein levels progressively declined

over time following CHX treatment, exhibiting a more pronounced decline compared to the H/R+siNC group (Fig. 5C). Therefore, YOD1 knockdown accelerates RIPK1 protein degradation via ubiquitination under H/R conditions.

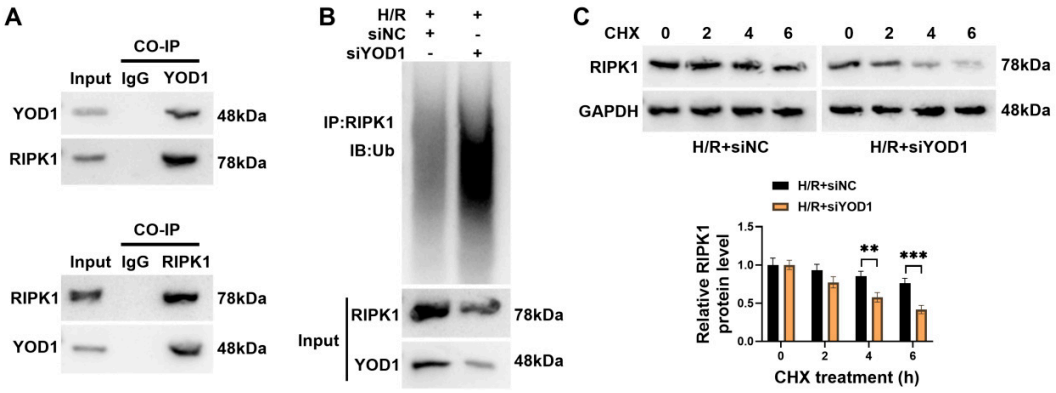

Figure 5: YOD1 inhibits the ubiquitination levels of RIPK1. (**A**) The interaction between YOD1 and RIPK1 was assessed by Co-IP. (**B**) The ubiquitination regulation of RIPK1 by YOD1 was assessed by a ubiquitination analysis experiment. (**C**) RIPK1 protein expression in AC16 cells with H/R+siNC and H/R+siYOD1 groups following CHX treatment at different times (0 h, 2 h, 4 h, and 6 h) was detected by western blotting assay. Data are presented as mean ± SD from three independent experiments (n = 3). $^{**}p < 0.01$, $^{***}p < 0.001$.

4 Discussion

Myocardial I/R injury remains a formidable challenge in ischemic heart disease management, contributing significantly to adverse cardiac outcomes despite timely reperfusion [24]. The intricate pathophysiological processes underlying I/R injury, including exacerbated inflammation, oxidative stress, and ferroptosis, are not yet fully elucidated [1]. Identifying key regulatory molecules is crucial for understanding this pathology.

This study demonstrated, through the validation using cellular models, that YOD1 exhibited a significant up-regulation trend in myocardial I/R injury *in vitro*. This finding aligns with previous reports indicating that members of the DUBs family are frequently activated by pathological stimuli (such as hypoxia and oxidative stress), participating in disease progression by regulating substrate stability [25]. For example, OTUD1 exacerbated neuroinflammation in Alzheimer's disease by deubiquitinating CCAAT/enhancer-binding protein β [26], whereas the overexpression of YOD1 might similarly reflect an adaptive (or pathological) response of cardiomyocytes to I/R injury. Studies have shown that in YOD1 knockdown mice, ISO-induced cardiac hypertrophy, fibrosis, and dysfunction are significantly alleviated [27]. In this study, YOD1 knockdown similarly alleviated H/R-induced decreases in cell viability and inflammatory cytokine secretion, suggesting that YOD1 promoted injury. Notably, YOD1 knockdown also improved oxidative stress and ferroptosis-associated alterations, two pathological processes closely associated with the severity of I/R injury [28,29]. Previous studies have demonstrated that ferroptosis can exacerbate membrane damage through lipid peroxidation products such as MDA, while ROS generated by oxidative stress can directly induce mitochondrial dysfunction [30,31]. The improvement observed in these indicators following YOD1 knockdown in this study suggests that it may exert its effects by regulating multiple pathological pathways.

Mechanistically, YOD1 knockdown significantly inhibited H/R-induced RIPK1 protein up-regulation and NF-κB pathway activation, as evidenced by decreased phosphorylation of p65 and IκBα, as well as reduced nuclear translocation of p65. As an upstream kinase of NF-κB, stable expression of RIPK1

activates IκBα degradation through IKKβ phosphorylation, thereby releasing p65 into the nucleus to initiate pro-inflammatory gene transcription [32,33]. RIPK1, a key regulator of cell survival, inflammation, and programmed necrosis (necroptosis), has been previously associated with I/R injury [34,35]. Additionally, the NF-κB pathway is a well-established master regulator of inflammation and cell survival, and its aberrant activation is a hallmark of I/R injury [36,37]. This research further validated the mediating role of RIPK1 through rescue experiments, demonstrating that overexpression of RIPK1 reversed the protective effects of YOD1 knockdown. This directly proves that YOD1 primarily influences cardiomyocyte fate by regulating RIPK1.

Studies have shown that RIPK1 is regulated by mitsugumin 53, undergoes deubiquitination and stable expression, and participates in necroptosis induced by myocardial I/R [19]. Herein, YOD1 knockdown significantly increased K63-linked ubiquitination of RIPK1, indicating that YOD1 primarily removed K63-linked polyubiquitin chains from RIPK1. Given that K63-linked ubiquitination could regulate protein stability and that ubiquitinated proteins were canonically degraded by the 26S proteasome, the CHX chase data further supported that YOD1 knockdown accelerated proteasome-dependent degradation of RIPK1. These findings collectively suggest that YOD1 suppresses the proteasomal degradation pathway of RIPK1 through deubiquitination modification, thereby maintaining its protein stability. This process aligns with the classic mode of action for DUBs, which stabilize target protein expression by deubiquitinating them and extending their half-life [38]. YOD1 likely stabilizes RIPK1 through a similar mechanism. Although this study has not directly tested a catalytically inactive YOD1 mutant, the observed physical interaction, increased ubiquitination upon YOD1 knockdown, and reduced protein half-life strongly support that YOD1's deubiquitinase activity is required for RIPK1 stabilization. Future studies using a catalytic mutant will further validate this conclusion.

In an *in vitro* H/R-induced cardiomyocyte model, this study identifies YOD1 as a potential pro-injury factor that promotes inflammation, oxidative stress, and ferroptosis-associated alterations through the "YOD1-RIPK1-NF-κB" axis. These findings offer preliminary mechanistic insights that may inform future studies on targeted interventions. If further validated *in vivo*, the development of small-molecule inhibitors for YOD1 could represent a novel strategy to mitigate myocardial I/R injury. Hence, this study has certain limitations: (I) All experiments were conducted exclusively in AC16 cells using an *in vitro* H/R model; no *in vivo* validation was performed. Therefore, the physiological relevance of these findings to intact myocardial I/R injury requires further confirmation using animal models (e.g., rat or mouse I/R models); (II) Upstream regulators of YOD1, such as whether HIF-1α participates in YOD1 up-regulation, were not thoroughly investigated; (III) The precise regulatory mechanisms of ferroptosis (such as whether YOD1 indirectly influences GPX4/ACSL4 via other molecules) require further refinement; (IV) Although this study assessed multiple classical ferroptosis-related indicators (GPX4, ACSL4, lipid ROS, MDA, and Fe^{2+}), functional rescue experiments using specific ferroptosis inhibitors or iron chelators were not performed. Therefore, the current findings more precisely reflect YOD1-mediated regulation of ferroptosis-associated alterations rather than definitive ferroptosis induction. Further validation using pharmacological inhibitors or genetic approaches is required to confirm the direct role of ferroptosis in this regulatory axis.

To sum up, this study illustrates that YOD1 plays a pro-injury role in H/R-induced cardiomyocytes by stabilizing RIPK1 and activating the NF-κB pathway. These observations point to YOD1 as a potential focus for further investigation into myocardial I/R injury, pending validation in *in vivo* models.

5 Conclusion

In conclusion, this research identifies YOD1 as a pro-injury factor in myocardial I/R injury induced by H/R. The current research demonstrates that YOD1 expression is up-regulated upon H/R stimulation, where it directly interacts with and deubiquitinates RIPK1. This deubiquitination stabilizes RIPK1 protein, leading to NF-κB signaling pathway activation. Consequently, this molecular axis exacerbates inflammatory responses, oxidative stress, and ferroptosis in cardiomyocytes, ultimately aggravating I/R-induced cellular injury. Conversely, knockdown of YOD1 effectively mitigates these pathological processes. These findings reveal a critical role of the YOD1/RIPK1/NF-κB axis in mediating myocardial I/R injury and position YOD1 as a potential therapeutic candidate for attenuating post-I/R cardiac damage.

Acknowledgement: None.

Funding Statement: The authors received no specific funding for this study.

Author Contributions: The authors confirm contribution to the paper as follows: Conceptualization, Zhen Liu; methodology, Xin Song; software, Xin Song; validation, Liangliang Liu; formal analysis, Linjun Wang; investigation, Zhen Liu; resources, Liangliang Liu; data curation, Xin Song; writing—original draft preparation, Liangliang Liu; writing—review and editing, Zhen Liu; visualization, Zhen Liu; supervision, Liangliang Liu; project administration, Liangliang Liu; funding acquisition, Zhen Liu. All authors reviewed and approved the final version of the manuscript.

Availability of Data and Materials: The data that support the findings of this study are available from the corresponding author, Zhen Liu, upon reasonable request.

Ethics Approval: Not applicable.

Conflicts of Interest: The authors declare no conflicts of interest.

Supplementary Materials: The supplementary material is available online at https://www.techscience.com/doi/10.32604/biocell.2026.080414/s1.

References

1. Fede MS, Daziani G, Tavoletta F, Montana A, Compagnucci P, Goteri G, et al. Myocardial ischemia/reperfusion injury: molecular insights, forensic perspectives, and therapeutic horizons. Cells. 2025;14(19):1509. [CrossRef].
2. Zhang M, Liu Q, Meng H, Duan H, Liu X, Wu J, et al. Ischemia-reperfusion injury: molecular mechanisms and therapeutic targets. Signal Transduct Target Ther. 2024;9(1):12. [CrossRef].
3. Tsurusaki S, Kizana E. Mechanisms and therapeutic potential of multiple forms of cell death in myocardial ischemia-reperfusion injury. Int J Mol Sci. 2024;25(24):13492. [CrossRef].
4. Hong J, Ye Y, Zheng D, Qian X. Kukoamine a activates Akt/GSK-3β pathway to repress oxidative stress and inflammation to alleviate myocardial ischemia-reperfusion injury. Lett Drug Des Discov. 2024;21(12):2374–83. [CrossRef].
5. Ahn JH, Won MH. Special issue "new molecular insights into ischemia/reperfusion". Int J Mol Sci. 2024;26(1):212. [CrossRef].
6. Huang X, Wang Y, Cui X, Yan Q, Xue T, Jing X. Insight into myocardial ischemia-reperfusion injury from the perspective of ferroptosis. Perfusion. 2025;40(5):1088–102. [CrossRef].
7. Han Z, Jia Q, Zhang J, Chen M, Wang L, Tong K, et al. Deubiquitylase YOD1 regulates CDK1 stability and drives triple-negative breast cancer tumorigenesis. J Exp Clin Cancer Res. 2023;42(1):228. [CrossRef].
8. Ernst R, Mueller B, Ploegh HL, Schlieker C. The otubain YOD1 is a deubiquitinating enzyme that associates with p97 to facilitate protein dislocation from the ER. Mol Cell. 2009;36(1):28–38. [CrossRef].
9. Zhao J, Guo X, Li H, Chen Y, Du J, Zhang J, et al. Regulation of disease signaling by YOD1: potential implications for therapeutic strategies. Cancer Cell Int. 2025;25(1):232. [CrossRef].

10. Liu J, Lu Y, Zhu R, Xi P, Yang Z, Zhang Z, et al. The deubiquitinase YOD1 suppresses tumor progression by stabilizing ZNF24 in clear cell renal carcinoma. Cell Death Dis. 2025;16:334. [CrossRef].
11. Sun J, Chen F, She L, Zeng Y, Tang H, Ye B, et al. YOD1 regulates microglial homeostasis by deubiquitinating MYH9 to promote the pathogenesis of Alzheimer's disease. Acta Pharm Sin B. 2025;15(1):331–48. [CrossRef].
12. Shen J, Lou L, Du X, Zhou B, Xu Y, Mei F, et al. YOD1 sustains NOD2-mediated protective signaling in colitis by stabilizing RIPK2. EMBO Rep. 2024;25(11):4827–45. [CrossRef].
13. Ye B, Lin W, Jiang Y, Zheng Z, Jin Y, Xu D, et al. Cardiomyocyte-derived YOD1 promotes pathological cardiac hypertrophy by deubiquitinating and stabilizing STAT3. Sci Adv. 2025;11(26):eadu8422. [CrossRef].
14. Mao H, Zhao X, Sun SC. NF-κB in inflammation and cancer. Cell Mol Immunol. 2025;22(8):811–39. [CrossRef].
15. Tan J. Preventive effect of alpha-pinene on cisplatin-induced kidney injury by oxidative stress, inflammation and apoptosis *via* NF-κB signaling pathway. Lett Drug Des Discov. 2024;21(12):2416–22. [CrossRef].
16. Dong P, Liu K, Han H. The role of NF-κB in myocardial ischemia/reperfusion injury. Curr Protein Pept Sci. 2022;23(8):535–47. [CrossRef].
17. Sun Z, Ye J, Sun W, Jiang L, Shan B, Zhang M, et al. Cooperation of TRADD- and RIPK1-dependent cell death pathways in maintaining intestinal homeostasis. Nat Commun. 2025;16(1):1890. [CrossRef].
18. Wang Y, Wang Z, Guo X, Tao Z, Wu C, Jiang M, et al. Empagliflozin attenuates DOX-induced cardiotoxicity by inhibiting RIPK1-mediated endoplasmic reticulum stress and autophagy. Biochim Biophys Acta BBA Mol Basis Dis. 2025;1871(6):167898. [CrossRef].
19. Wang Q, Park KH, Geng B, Chen P, Yang C, Jiang Q, et al. MG53 inhibits necroptosis through ubiquitination-dependent RIPK1 degradation for cardiac protection following ischemia/reperfusion injury. Front Cardiovasc Med. 2022;9:868632. [CrossRef].
20. Ma X, Xie J, Li B, Shan H, Jia Z, Liu W, et al. Weighted gene co-expression network analysis and single-cell sequence analysis uncover immune landscape and reveal hub genes of necroptosis in macrophages in myocardial ischaemia–reperfusion injury. Int Immunopharmacol. 2024;140:112761. [CrossRef].
21. Song Z, Ye L, Wang Y, Wang W, Liu C, Lu J, et al. Targeting RIPK1-mediated necroptosis, oxidative stress, and ferroptosis: a novel multitarget therapy for ischemic stroke. Eur J Med Chem. 2025;296:117884. [CrossRef].
22. Hafez P, Chowdhury SR, Jose S, Law JX, Ruszymah BHI, Mohd Ramzisham AR, et al. Development of an *in vitro* cardiac ischemic model using primary human cardiomyocytes. Cardiovasc Eng Technol. 2018;9(3):529–38. [CrossRef].
23. Zhang J, Jiang S, Lu C, Pang J, Xu H, Yang F, et al. SYVN1/GPX5 axis affects ischemia/reperfusion induced apoptosis of AC16 cells by regulating ROS generation. Am J Transl Res. 2021;13(5):4055–67.
24. Ghanta SN, Kattamuri LPV, Odueke A, Mehta JL. Molecular insights into ischemia-reperfusion injury in coronary artery disease: mechanisms and therapeutic implications: a comprehensive review. Antioxidants. 2025;14(2):213. [CrossRef].
25. Lange SM, Armstrong LA, Kulathu Y. Deubiquitinases: from mechanisms to their inhibition by small molecules. Mol Cell. 2022;82(1):15–29. [CrossRef].
26. She LY, Li LY, Tang H, Yu Q, Gao FY, Zeng YQ, et al. OTUD1 positively regulates microglia neuroinflammation and promotes the pathogenesis of Alzheimer's disease by deubiquitinating C/EBPβ. Acta Pharmacol Sin. 2025;46(10):2608–21. [CrossRef].
27. Zheng QS, Xiong YQ, Xu JC, Qian JF, Luo W, Wang QY, et al. YOD1 mediates isoproterenol-induced cardiac remodeling by deubiquitinating PKM2 and reducing PKM2 tetramerization in cardiomyocytes. Acta Pharmacol Sin. 2025;46(11):2938–50. [CrossRef].
28. Wang X, Chen T, Chen S, Zhang J, Cai L, Liu C, et al. STING aggravates ferroptosis-dependent myocardial ischemia-reperfusion injury by targeting GPX4 for autophagic degradation. Signal Transduct Target Ther. 2025;10:136. [CrossRef].
29. Mastoor Y, Murphy E, Roman B. Mechanisms of postischemic cardiac death and protection following myocardial injury. J Clin Investig. 2025;135(1):e184134. [CrossRef].
30. Dhalla NS, Ostadal P, Tappia PS. Involvement of oxidative stress and antioxidants in modification of cardiac dysfunction due to ischemia-reperfusion injury. Antioxidants. 2025;14(3):340. [CrossRef].
31. Li W, Liao Y, Chen J, Kang W, Wang X, Zhai X, et al. Ischemia—Reperfusion injury: a roadmap to precision therapies. Mol Aspects Med. 2025;104:101382. [CrossRef].

32. Milosevic M, Magnutzki A, Braun T, Hussain S, Jakschitz T, Kragl M, et al. Anti-inflammatory and cytoprotective polypharmacology of Canephron N reveals targeting of the IKK-NF-κB and p38-MK2-RIPK1 axes. Biomed Pharmacother. 2025;182:117747. [CrossRef].
33. Cai Z, Wang H, Han F, Wang J, Lv H, Gao XJ, et al. Zinc deficiency induces hepatic oxidative stress, inflammation, and programmed cell death in mice. Biol Trace Elem Res. 2026;204(2):893–908. [CrossRef].
34. Fischer FA, Demarco B, Min FCH, Yeap HW, De Nardo D, Chen KW, et al. TBK1 and IKKε prevent premature cell death by limiting the activity of both RIPK1 and NLRP3 death pathways. Sci Adv. 2025;11(10):eadq1047. [CrossRef].
35. Liu T, Huang G, Guo X, Ji Q, Yu L, Zong R, et al. The protein arginine methyltransferase PRMT1 ameliorates cerebral ischemia–reperfusion injury by suppressing RIPK1-mediated necroptosis and apoptosis. Acta Pharm Sin B. 2025;15(8):4014–29. [CrossRef].
36. Shuang L, Su Y, Zhang Y. Downregulation of Gldc attenuates myocardial ischemia reperfusion injury *in vitro* by modulating Akt and NF-κB signalings. Sci Rep. 2025;15:268. [CrossRef].
37. Tian K, Song L, Liu L, Lai T, Liu W. Rutin protects myocardial ischemia-reperfusion injury *via* the NF-κB/NLRP3/pyroptosis pathway. ACS Omega. 2025;10(21):21777–85. [CrossRef].
38. Su JB, Chen G, Sun QY, Fu X, Wu LX, Qiu HB, et al. USP48 protects against myocardial ischemia-reperfusion injury by stabilizing and upregulating CNN1 in type 1 diabetes mice. Metabolism. 2025;170:156326. [CrossRef].